Fluid Inertia Effects in Squeeze Film Dampers

A. El-Shafei

Assistant Professor
Department of Mechanical Engineering
University of South Florida
Tampa, FL 33620

Abstract

Fluid inertia effects in squeeze film dampers are investigated. An approximate energy method, based on the assumption that the velocity profiles of the classical lubrication theory do not change much due to fluid inertia, is used. The kinetic coenergy of the fluid is calculated and the inertia forces are obtained by Lagrange's equations in conjunction with Reynolds transport theorem. The governing equations are then solved for a small circular centered whirl. It is shown that for this case the fluid inertia forces are equal to the viscous forces in the damper at squeeze Reynolds number equal to 10, and are larger thereafter. It is also shown that the added mass due to fluid inertia can be as high as 60 times the mass of the journal and thus cannot be neglected in the dynamic analysis of rotors incorporating squeeze film dampers. Also, it is shown that the classical lubrication theory is in error with respect to the pressure field and inertia forces, but predicts the velocity field reasonably accurately, for Reynolds number within the range of usual application of squeeze film dampers.

Introduction

Squeeze film dampers (SFDs) are damping devices used in gas turbine engines to damp the whirling vibration of rotors. Their ability to attenuate the amplitude of engine vibrations and to decrease the magnitude of the force transmitted to the engine frame makes them an attractive rotor support. Also, the energy removed in the dampers enhances the stability of the rotor-bearing system.

SFDs are usually designed based on Reynolds equation of the classical lubrication theory, which neglects the effects of fluid inertia. Recently, in their experiments on SFDs Tecza, *et. al.* [9] showed that fluid inertia may be a significant factor in determining the dynamic characteristics of SFDs. They encountered a critical speed in their experimental rig which they did not expect from their rotordynamic analysis. They attributed this critical to fluid inertia. This has prompted several investigations of the effects of fluid inertia in SFDs. Tichy[10] provided an explanation for the importance of fluid inertia in SFDs versus journal bearings. San Andrés and Vance[6] obtained the steady state response of a rotor incorporating SFDs, including fluid inertia effects by using an averaged momentum approximation.[5]

Perhaps one of the first attempts to study the effects of fluid inertia in hydrodynamic bearings, is the work of Smith.[7] Using a unique form of Reynolds equation, he was able to obtain inertia force coefficients for journal bearings, and his conclusion was that the effect of fluid inertia in oil film bearings is to introduce an added mass to the rotor and this may affect the dynamics of the rotor especially for short stiff rotors on wide bearings. Approximately a decade later Reinhardt and Lund[4] used a perturbation solution for small Reynolds number to obtain the force coefficients of journal bearings. They showed that fluid inertia introduces rather small corrections to the damping and stiffness coefficients of journal bearings and they also provided plots of inertia coefficients versus the eccentricity. They had to solve a set of differential equations numerically to arrive at these plots. Another notable paper, is the work of Szeri *et. al.* [8] They used a technique based on averaging the inertia forces across the film, to obtain the force coefficients in a squeeze film damper. They also had to solve the resulting differential equations numerically. A recent paper by Ramli *et. al.*[3] compares the results of Smith, Reinhardt and Lund, and Szeri *et. al.*; and concludes that they are in good agreement, especially for short bearings. It is pointed out, however, that Smith's approach has the advantage of computational simplicity, and leads to fairly simple asymptotic analytical expressions for very short, and very long bearings.

Here, we will show that for a SFD whose journal executes a small circular-centered whirl, the fluid inertia forces are equal to the viscous forces in the damper at squeeze Reynolds number equal to 10, and are larger thereafter. We will also show that for Reynolds number in the range of usual application of SFDs, the velocity profiles do not change much due to fluid inertia. That is, the classical lubrication theory is in error with respect to the pressure field and inertia forces, but predicts the velocity field reasonably accurately.

A recently developed model of fluid inertia in SFDs[1], is based on the assumption that the velocity field predicted by the classical lubrication theory is not changed much by fluid inertia. This permits the kinetic coenergy of the fluid to be calculated, and the inertia forces to be obtained by Lagrange's equations as applied to an open system. This energy approximation has the advantage of the applicability to cavitated dampers, since it is essentially a control volume approach, and consequently can handle the free surfaces that arise due to cavitation. This model is used in this paper to predict the fluid inertia forces in SFDs whose journal execute a large amplitude orbit. The damping forces in the SFDs are obtained by Reynolds equation.

Squeeze Film Dampers

Figure 1 shows the construction of squeeze film dampers. In a typical application, the damper consists of an oil film in an annulus surrounding a rolling element bearing whose outer race is constrained from rotating, usually by a squirrel cage. Thus the spinning of the rotor does not reach the oil, and only when the rotor whirls does the oil film act to damp the motion. The squirrel cage serves to center the journal in the sleeve as well as to keep the outer race of the rolling element bearing from spinning.

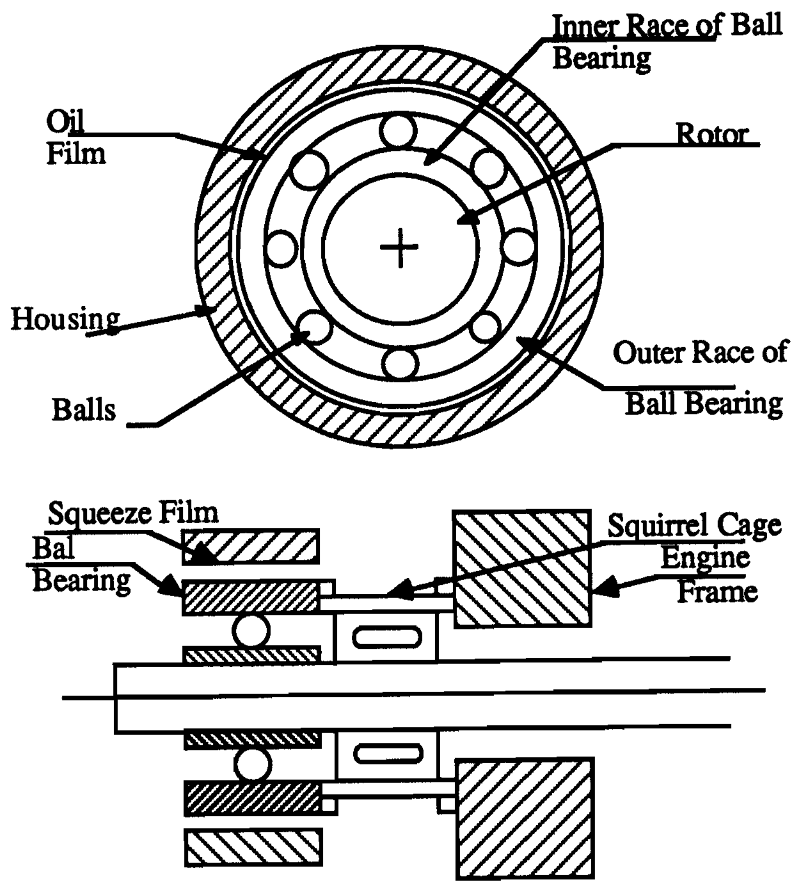

Figure 1 Construction of squeeze film dampers

Figure 2 shows a SFD, and the coordinate systems used. The film thickness h at any given location is given by

$$h = c - e \cos \theta \tag{1}$$

where c is the clearance, e is the eccentricity of the journal and θ is measured from the positive r-axis of the whirling coordinate system (r, t, z). The z-axis is perpendicular to the plane of the paper. Also shown in Figure 2, the stationary coordinate system (x, y, z) and the angle φ which is measured from the positive x-axis, and $\theta = \varphi - \psi$. For a steady circular whirl $\psi = \omega t$, where ω is the whirling frequency of the journal and t is time. The flow in the damper is described with respect to the stationary coordinate system (X, Y, Z) shown in Figure 2.

In SFDs the ratio of the clearance c to the radius R is of the order of 10^{-3}, such that the effects of curvature can be neglected, and we can use the stationary cartezian (X, Y, Z)

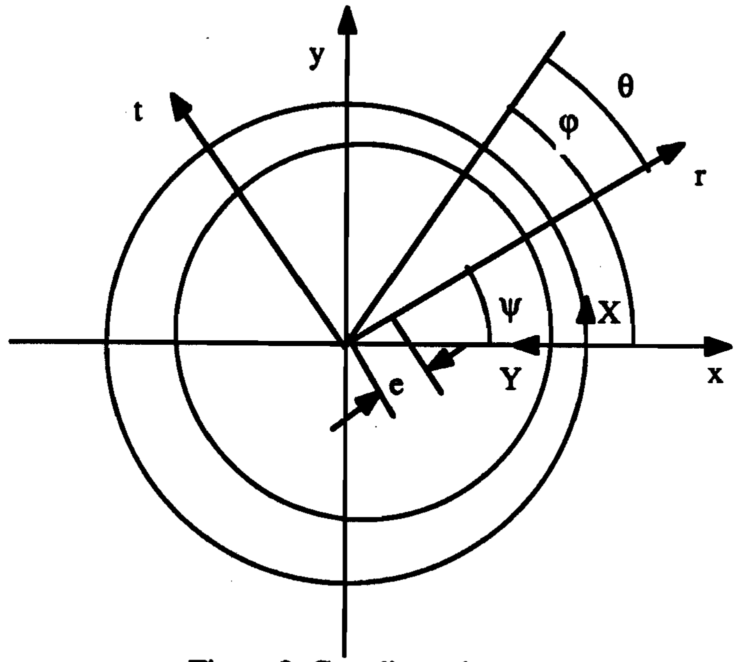

Figure 2 Coordinate frames

coordinate system shown in Figure 2, (with the Z-axis perpendicular to the plane of the paper), to describe the flow. To an observer in this coordinate system, because c/R is small, it appears as if the damper is unwrapped, as shown in Figure 3. The upper surface in Figure 3 represents the journal, while the lower surface represents the bearing. The motion of the journal, i.e. the upper surface in Figure 3, results in the motion of the fluid in the clearance between the two surfaces. Due to the motion of the journal, the upper surface in Figure 3 travels in a wave-like fashion, and also changes its shape if the journal is moving radially. It should be noted that since the flow in the damper is cyclic, i.e. the conditions at $\varphi = 0$ are the same as those at $\varphi = 2\pi$, then the model of Figure 3 is repeated every $2\pi R$ in the X-direction.

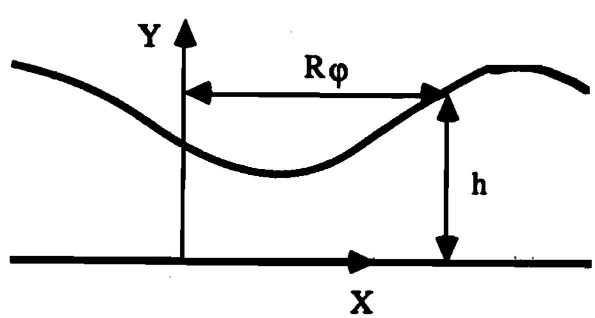

Figure 3 Unwrapped squeeze film damper

The damping forces in SFDs are obtained by the solution of Reynolds equation for fluid lubrication. There are two mathematical approximations to Reynolds equation, that have physical significance, namely the short bearing approximation and the long bearing approximation. In the short bearing approximation to Reynolds equation, which is justified if the damper is short in the axial direction, the flow in the damper is axial rather than circumferential, and thus the axial pressure gradient is much larger than the circumferential pressure gradient. On the other hand, in the long bearing approximation to Reynolds equation, which is justified if the damper is long in the axial direction, the flow in the damper is circumferential, and thus the circumferential pressure gradient is much larger than the axial pressure gradient. In practice, if the damper is tightly sealed, then the flow is circumferential even if the dampers are physically short. In this case, the long bearing approximation would describe the conditions in the damper better than the short bearing approximation.

Integrating the pressure obtained by the solution of Reynolds equation, we obtain the damping forces in SFDs, which take the form

$$F_{rc} = -C_{rr}\,\dot{e} - C_{rt}\,e\,\dot{\psi} \tag{2}$$

$$F_{tc} = -C_{tr}\,\dot{e} - C_{tt}\,e\,\dot{\psi} \tag{3}$$

Damping Coefficients - Short Bearing

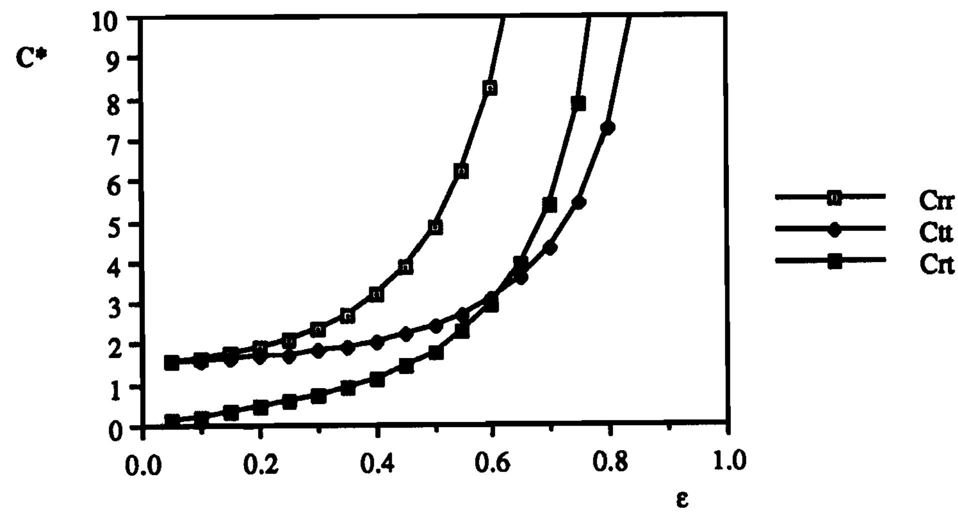

Damping Coefficients - Long Bearing

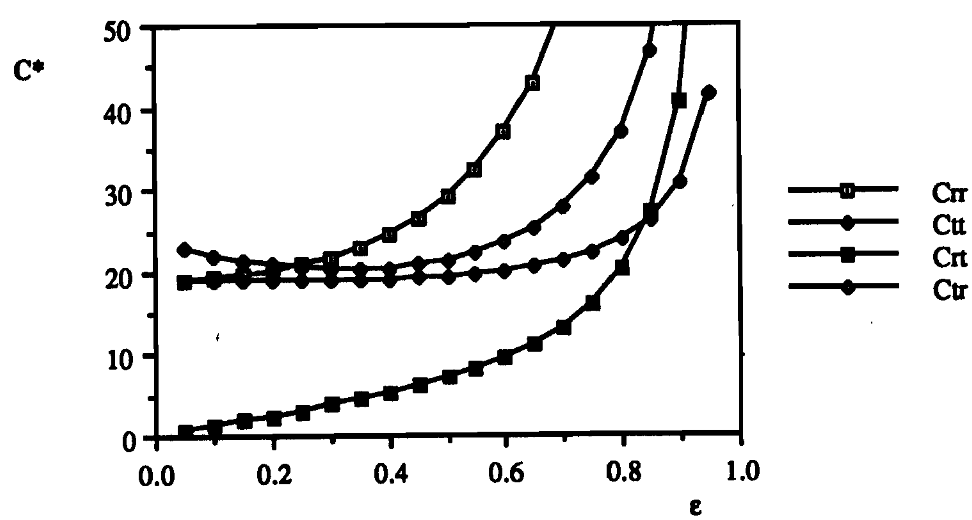

Figure 4 Damping coefficients (nondimensional) vs ε

where F_{rc} and F_{tc} are the radial and tangential damping forces, respectively, and $\dot{e}$ and $e\,\dot{\psi}$ are the radial and tangential velocities, respectively. The damping coefficients C_{rr}, C_{tt}, C_{tr} and C_{rt} are in general nonlinear functions of the position and velocity of the journal in the damper. Figure 4 shows a plot of the damping coefficients C_{rr}, C_{tt}, C_{tr} and C_{rt} versus the eccentricity ratio ε, which is defined as the ratio e/c, for a cavitated damper using the π-film theory and nearly circular-centered whirl. It can be seen from Figure 4 that the damping coefficients for the short and long bearing approximations are nonlinear functions of the position of the journal in the damper. In fact, the damping coefficients increase as the eccentricity increases, and this, in one sense, is a desirable characteristic, since the damper provides more damping as the amplitude of the whirl increases which is obviously beneficial. Perhaps, this is why squeeze film dampers are such effective damping devices. On the other hand, it is precisely this nonlinear characteristic that results in the nonlinear behavior of the rotor-bearing system (jump resonance, subharmonic motion, ... etc.). Note that, in Figure 4, the damping coefficients C_{rt} and C_{tr} are equal for the short bearing.

Fluid Inertia Forces in SFDs

To calculate the fluid inertia forces in the damper for a general orbit, it would be nearly impossible to solve the governing equations analytically, except in very special cases. Thus we have to resort to an approximate method to estimate the fluid inertia forces in the damper. We are going to use the energy method developed by El-Shafei[1], which relies on the assumption that the velocity profiles in the damper can be approximated by the solution of the classical lubrication theory, which will be shown to be a valid assumption in the next section. This permits the kinetic coenergy of the fluid to be calculated, and the inertia forces to be obtained by Lagrange's equations as applied to an open system.

For a short damper, the axial velocity profile predicted by the classical lubrication theory is given by

$$w = \frac{6\,z}{h}\left(\frac{Y}{h} - \frac{Y^2}{h^2}\right)(\,e\,\dot{\psi}\sin\theta + \dot{e}\cos\theta\,) \tag{4}$$

while for a long damper the circumferential velocity profile predicted by the classical lubrication theory is given by

$$u = \frac{6\,R}{h}\left(\frac{Y}{h} - \frac{Y^2}{h^2}\right)\left[\,\sin\theta\,\dot{e} - \cos\theta\,e\,\dot{\psi} + \frac{3\,\varepsilon}{(\,2+\varepsilon^2\,)}\,e\,\dot{\psi}\,\right] \tag{5}$$

and thus the kinetic coenergy of the fluid in the damper, which is defined by

$$T^* = \frac{1}{2}\int_{\theta_1}^{\theta_2}\int_0^h\int_{-\frac{L}{2}}^{\frac{L}{2}} \rho\,(u^2 + v^2 + w^2)\,R\,d\theta\,dY\,dZ \tag{6}$$

where ρ is the density of the fluid, R is the radius of the damper and L is its length. Thus the kinetic coenergy of the fluid in the damper can be calculated as

$$T^* = \frac{1}{2}\,m_{rr}\,\dot{e}^2 + \frac{1}{2}\,m_{tt}\,(e\dot{\psi})^2 + m_{rt}\,\dot{e}\,e\dot{\psi} \tag{7}$$

where m_{rr}, m_{tt} and m_{rt} represent the inertia coefficients of the damper. For a cavitated damper we are also going to assume the π-film theory[2], while for an uncavitated damper we will have a full film, i.e. a 2π-film.

The inertia forces in the damper can be obtained by Lagrange's equations, but since the damper is an open system (because of the fluid being squeezed out axially), Reynolds transport theorem[1] must be used in conjunction with Lagrange's equations. Thus the radial and tangential inertia forces become

$$F_{i,r} = F_{ri} + R_{ri} \tag{8}$$

and

$$F_{i,t} = F_{ti} + R_{ti} \tag{9}$$

where $F_{i,r}$ is the radial inertia force and $F_{i,t}$ is the tangential inertia force, R_{ri} and R_{ti} are the inertia forces due to the flux of the fluid particles across the control surface, in the r- and t- directions, respectively, and F_{ri} and F_{ti} are obtained by Lagrange's equations and are given by

$$F_{ri} = -\frac{d}{dt}\left(\frac{\partial T^*}{\partial \dot{e}}\right) + \frac{\partial T^*}{\partial e} \tag{10}$$

and

$$F_{ti} = -\frac{1}{e}\frac{d}{dt}\left(\frac{\partial T^*}{\partial \dot{\psi}}\right) + \frac{1}{e}\frac{\partial T^*}{\partial \psi} \tag{11}$$

The flux terms R_{ri} and R_{ti} are given by

$$R_{ri} = -\int_{cs} \frac{\partial t^*}{\partial \dot{e}} \mathbf{V} \cdot \mathbf{n} \; dS + \int_{cs} t^* \frac{\partial (\mathbf{V} \cdot \mathbf{n})}{\partial \dot{e}} dS$$

$$R_{ti} = -\frac{1}{e}\int_{cs} \frac{\partial t^*}{\partial \dot{\psi}} \mathbf{V} \cdot \mathbf{n} \; dS + \frac{1}{e}\int_{cs} t^* \frac{\partial (\mathbf{V} \cdot \mathbf{n})}{\partial \dot{\psi}} dS$$

where t^* is the kinetic coenergy per unit volume, $\mathbf{V}$ is the velocity of the fluid with respect to the control surface S, $\mathbf{n}$ is the outward normal vector on the control surface. On calculating the above equations, for a 2π-film, with the journal executing a circular centered whirl, we get for the radial and tangential forces (including the damping forces)

$$F_r = m_r\, e\, \dot{\psi}^2 - C_{rt}\, e\, \dot{\psi} \tag{12}$$

$$F_t = -\, m_t\, e\, \dot{\psi}^2 - C_{tt}\, e\, \dot{\psi} \tag{13}$$

where for a short damper the coefficients are given by

$$m_r = \frac{\rho R L^3}{70\, c}\, \frac{2\pi}{\varepsilon^2}\left[\, 27 - \frac{(27 - 17\,\varepsilon^2)}{(1-\varepsilon^2)^{1/2}}\right]$$

$$C_{tt} = \frac{\mu R L^3}{c^3}\, \frac{\pi}{(1-\varepsilon^2)^{3/2}}$$

while for a long damper the coefficients are given by

$$m_r = \frac{12}{10}\, \frac{\rho R^3 L}{c}\left\{\frac{4\pi}{(2+\varepsilon^2)^2}\left[\, 6 - \frac{(10-\varepsilon^2)(1-\varepsilon^2)^{1/2}}{(2+\varepsilon^2)}\right]\right\}$$

$$C_{tt} = \frac{\mu R^3 L}{c^3}\, \frac{24\pi}{(2+\varepsilon^2)(1-\varepsilon^2)^{1/2}}$$

where μ is the viscosity of the fluid. For a 2π-film, the coefficients m_t and C_{rt} are zero for both the long and short dampers. The above inertia coefficients are plotted in Figure 5 for a 2π-film, for the short damper and for the long damper.

This model of fluid inertia was used by El-Shafei[1,2] to determine the unbalance response of Jeffcott rotors incorporating squeeze film dampers. Cavitated dampers were considered and the π-film theory was used. The results presented in the above mentioned references indicate that, in general, the effects of fluid inertia on the dynamics of the rotor are beneficial. Fluid inertia resulted in the decrease of the possibility of the jump resonance for the short damper, and resulted in better attenuation of the amplitude response at the critical speed. However, fluid inertia introduced an additional critical speed for the Jeffcott rotor, and this resulted in the decrease of the range of good vibration isolation for the dampers. Also, it was found that in general the long dampers are better at attenuating the amplitude response of the engine, while the short dampers are better at attenuating the magnitude of the force transmitted to the engine frame.

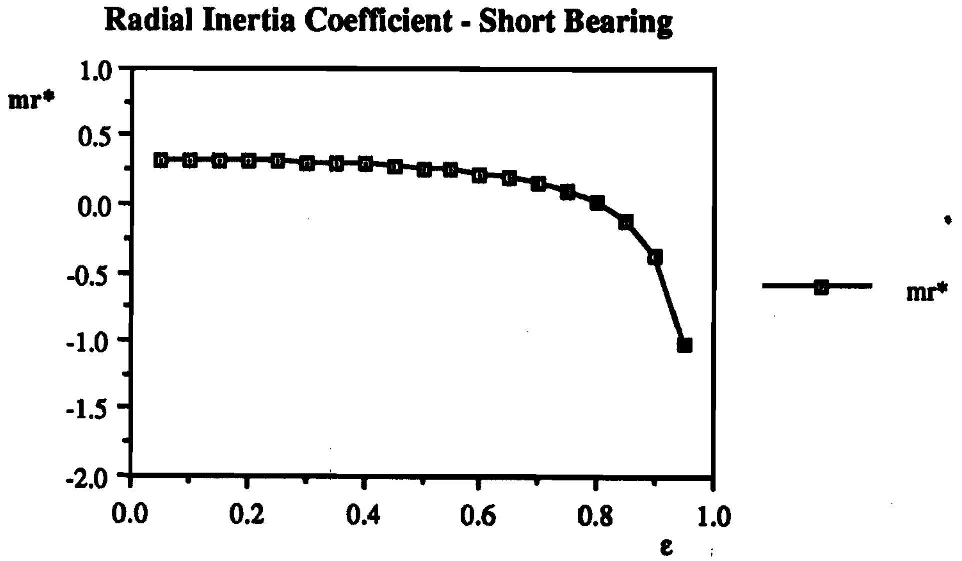

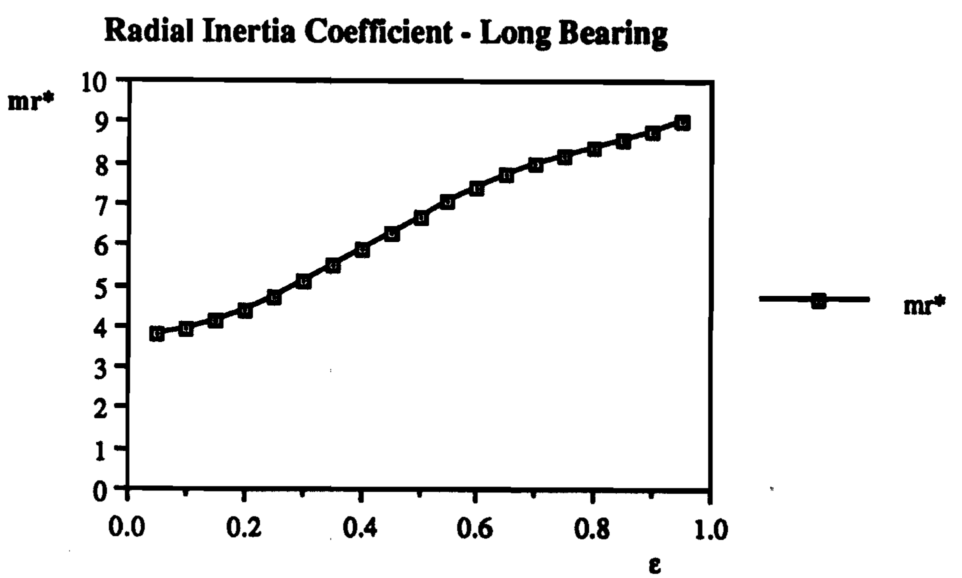

Figure 5 Inertia coefficients (nondimensional) vs ε

Small Circular Centered Whirl

For a small circular centered whirl, that is with $e << c$, the convective acceleration terms in the Navier-Stokes equations can be neglected, and the governing equations for the flow in the damper become

$$\frac{\partial u}{\partial t} = -\frac{1}{\rho}\frac{\partial p}{\partial X} + \nu \frac{\partial^2 u}{\partial Y^2} \tag{14}$$

$$\frac{\partial p}{\partial Y} = 0 \tag{15}$$

$$\frac{\partial w}{\partial t} = -\frac{1}{\rho}\frac{\partial p}{\partial Z} + \nu \frac{\partial^2 w}{\partial Y^2} \tag{16}$$

and

$$\frac{\partial u}{\partial X} + \frac{\partial v}{\partial Y} + \frac{\partial w}{\partial Z} = 0 \tag{17}$$

where ν is the kinematic viscosity of the fluid, u is the velocity of the fluid in the X-direction, v is the velocity of the fluid in the Y-direction, w is the velocity of the fluid in the Z-direction, and p is the pressure. Furthermore, the boundary conditions on the upper surface of Figure 3, can be satisfied on the average. Thus the boundary conditions that equations (14-17) have to satisfy are

$$\begin{array}{lllll} \text{At} & y=0 & u=0 & v=0 & w=0 \\ \text{At} & y=c & u=U & v=V & w=0 \end{array} \tag{18}$$

where, for a circular whirl U and V are given by

$$U = \text{Real}\{\, e\,\omega\, e^{i\theta} \,\}$$

$$V = \text{Real}\{\, i\, e\,\omega\, e^{i\theta} \,\}$$

where $i = (-1)^{1/2}$ and $\omega = \dot{\psi}$ is the frequency of the whirl. In this case $\theta = \varphi - \omega t$ which suggests that the upper surface of Figure 3, travels like a wave, and thus we should seek a solution in the form

$$u = U_0\, e^{i\theta} \qquad v = V_0\, e^{i\theta} \qquad w = W_0\, e^{i\theta} \qquad p = P_0\, e^{i\theta} \tag{19}$$

where U_0, V_0 and W_0 are functions of Y and Z, while P_0 is a function of Z only. Substituting (19) into (14), we get

$$\frac{d^2 U_0}{dY^2} + \frac{i\,\rho\,\omega}{\mu} U_0 = \frac{i}{\mu R} P_0$$

which can be solved for U_0 using the boundary conditions (18), thus, neglecting terms of O(c/R), we get

$$U_0 = \frac{P_0}{\rho\,\omega\, R}\left[\frac{\sinh(s(Y-c)) - \sinh(sY) + \sinh(sc)}{\sinh(sc)}\right] \tag{20}$$

where

$$s = \frac{1}{c}\sqrt{\frac{Re}{2}}\,(1-i)$$

and $Re = \rho\,\omega\, c^2/\mu$ is the squeeze Reynolds number. Substituting (19) into (16), we get

$$\frac{d^2W_0}{dY^2} + \frac{i\rho\omega}{\mu} W_0 = \frac{1}{\mu}\frac{dP_0}{dZ}$$

which can be solved for W_0 using the boundary conditions (18), thus

$$W_0 = -\frac{i}{\rho\omega}\frac{dP_0}{dZ}\left[\frac{\sinh(s(Y-c)) - \sinh(sY) + \sinh(sc)}{\sinh(sc)}\right] \quad (21)$$

Substituting (19), (20) and (21) into the continuity equation, equation (17), we get

$$\frac{\partial V_0}{\partial Y} = \frac{i}{\rho\omega}\left(\frac{d^2P_0}{dZ^2} - \frac{1}{R^2}P_0\right)\left[\frac{\sinh(s(Y-c)) - \sinh(sY) + \sinh(sc)}{\sinh(sc)}\right]$$

The above equation can be integrated over Y and using the boundary condition $V_0 = 0$ at $Y=0$, we get

$$V_0 = \frac{i}{\rho\omega}\left(\frac{d^2P_0}{dZ^2} - \frac{1}{R^2}P_0\right)\left[\frac{\cosh(s(Y-c)) - \cosh(sY) + sY\sinh(sc) + 1 - \cosh(sc)}{s\sinh(sc)}\right]$$

The other boundary condition that V_0 has to satisfy, namely, at $Y=c$ the velocity $V_0 = i\,e\,\omega$, gives us

$$\frac{d^2P_0}{dZ^2} - \frac{1}{R^2}P_0 = \frac{\rho e \omega^2}{c}\left[\frac{sc\sinh(sc)}{2 - 2\cosh(sc) + sc\sinh(sc)}\right] \quad (22)$$

which is a differential equation that the pressure P_0 has to satisfy together with the boundary conditions

$P_0 = 0$ at $Z = \pm L/2$

and on solving (22) we get

$$P_0 = \frac{\rho e \omega^2 R^2}{c}\left[\frac{sc\sinh(sc)}{2 - 2\cosh(sc) + sc\sinh(sc)}\right]\left\{\frac{\cosh\left(\frac{2Z}{D}\right)}{\cosh\left(\frac{L}{D}\right)} - 1\right\} \quad (23)$$

where $D = 2R$ is the diameter of the damper. Equation (23) is a finite length solution for the pressure P_0 in a squeeze film damper whose journal executes a small circular-centered whirl, which is valid for all Re (in the laminar regime).

If we substitute the pressure from equation (23) into equations (20) and (21) we will get the velocity profiles in the damper. If we take the limit as $L/D \to 0$, i.e. the short damper case, the axial velocity profiles, for $Z = L/4$, $R = 1.25$ in., $c = 8$ mils and $\theta = 1$ rad, are shown in Figure 6 for various Re. Plotted on the same figure is the velocity profile obtained by the classical lubrication theory for a short damper. SFDs usually operate at Reynolds number of the order of 20, and it can be seen from Figure 6 that the velocity profiles of short SFDs do not change much due to fluid inertia, in the range of usual application of SFDs.

If we take the limit of the velocity profiles as $L/D \to \infty$, i.e. the long damper case, the circumferential velocity profiles, for the same data as Figure 6, are shown in Figure 7 for various Re. Also plotted on the Figure 7 is the velocity profile obtained by the classical lubrication theory for a long damper. Although the velocity profiles of the long dampers are more sensitive to Re than those of the short damper, yet it may be concluded that also for the long dampers, in the range of usual application of SFDs, the velocity profiles do not change much due to fluid inertia.

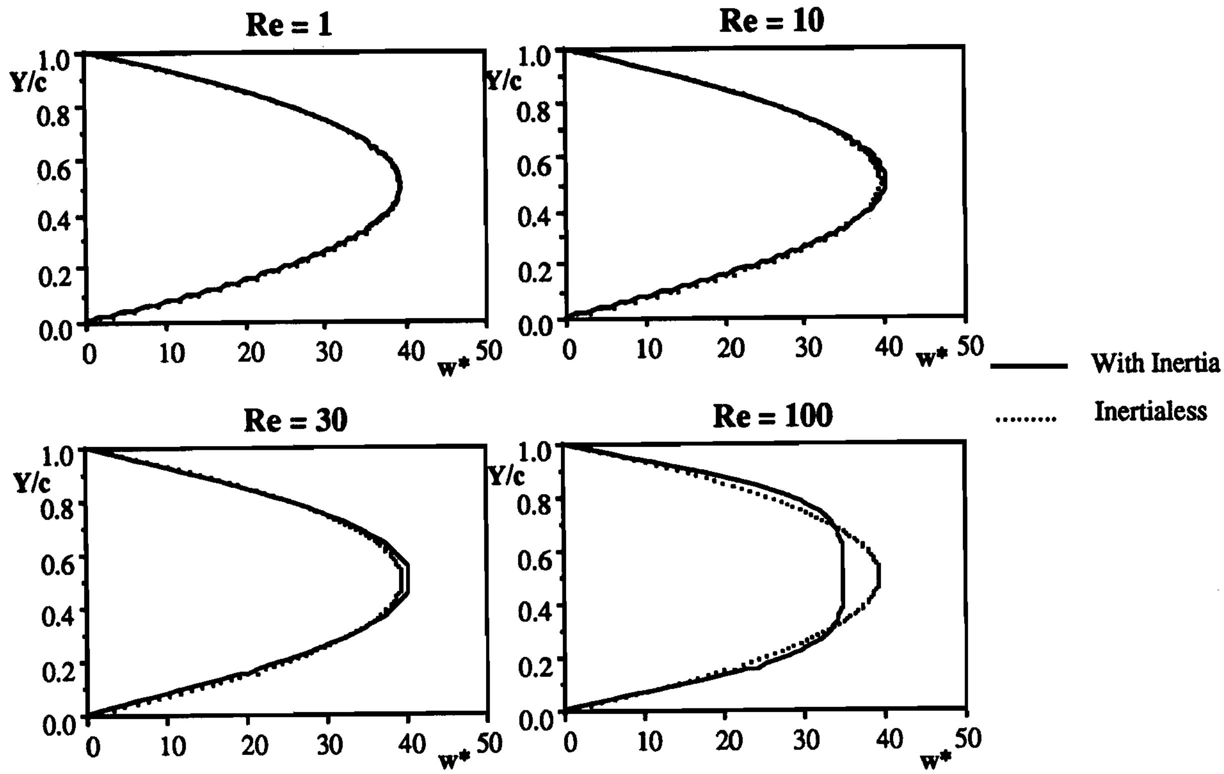

Figure 6 Velocity profiles - Short bearing (nondimensional)

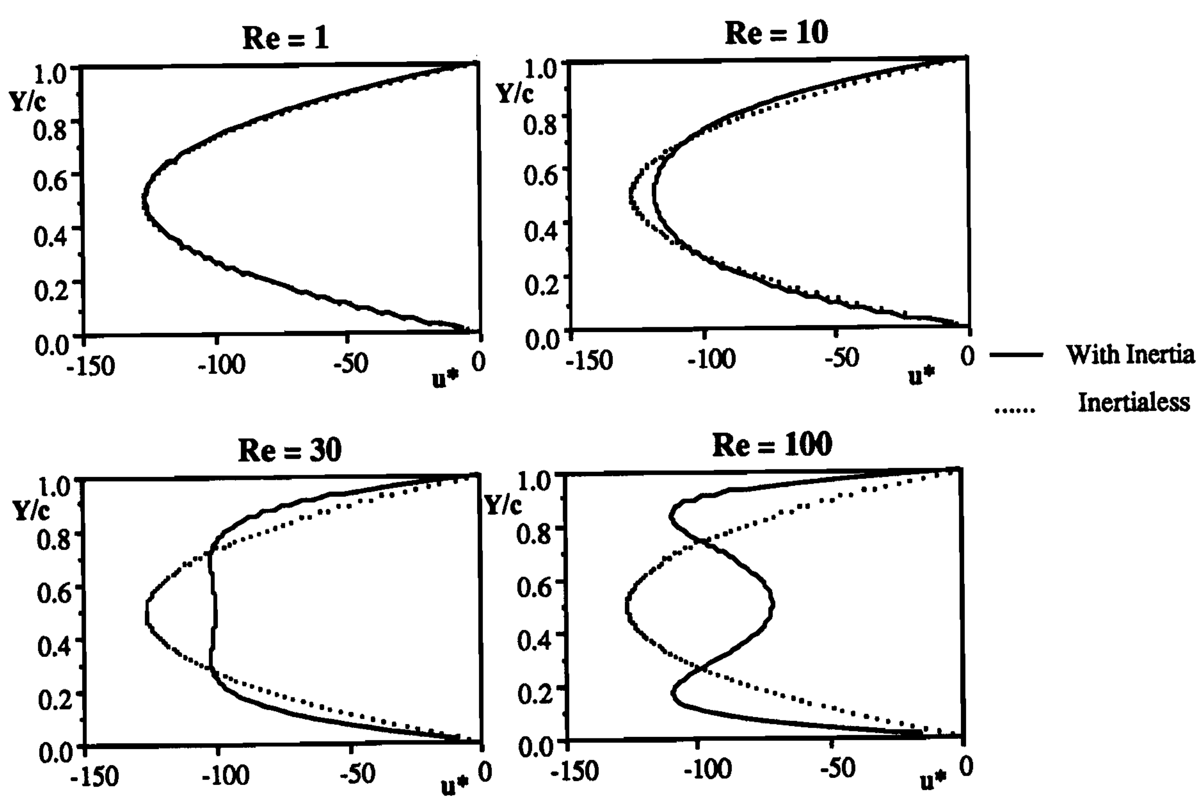

Figure 7 Velocity profiles - Long bearing (nondimensional)

The pressure in the damper is given by

$$p = \text{Real}\left\{ \left[\frac{\rho\, e\, \omega^2 R^2}{c} \; \frac{s\,c \sinh(s\,c)}{2 - 2\cosh(sc) + sc \sinh(sc)} \right] \left[\frac{\cosh\left(\frac{2Z}{D}\right)}{\cosh\left(\frac{L}{D}\right)} - 1 \right] e^{i\theta} \right\} \tag{24}$$

The pressure in equation (24) depends on Re only through the terms inside the first square bracket, namely

$$f(\text{Re}) = \left[\frac{\rho\, e\, \omega^2 R^2}{c} \; \frac{s\,c \sinh(s\,c)}{2 - 2\cosh(sc) + sc \sinh(sc)} \right] \tag{25}$$

If we take the limit as Re → 0 of equation (25) we get

$$\lim_{\text{Re}\to 0} f(\text{Re}) = \frac{12 R^2 \mu\, e\, \omega}{c^3} \left(i + \frac{\text{Re}}{10} \right) \tag{26}$$

Figure 8 shows a plot of the real and imaginary parts of f(Re) versus Re as predicted from equation (25). Also plotted on Figure 8 are the real and imaginary parts of the limit of f(Re)

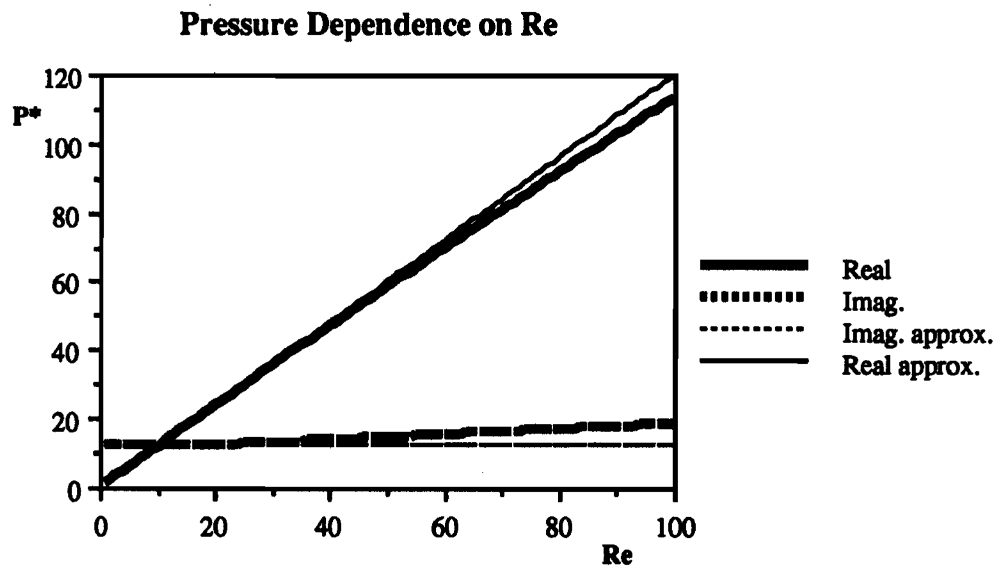

Figure 8 Nondimensional pressure vs. Re

as Re → 0, equation (26), from which it is clear that equation (26) is a good approximation of equation (25) for Re up to about 50. If we make an analogy with a mass dashpot system, it can be shown that the imaginary parts of equations (25) and (26) represent the contribution of the viscous force, while the real parts of equations (25) and (26) represent the contribution of the inertia force. In fact, the imaginary part of the approximation of equation (26) is equal to the contribution of the viscous force as predicted by the classical lubrication theory, and the real part of the approximation of equation (26) is equal to the contribution of the inertia force as predicted by the energy method described in the previous section.[1] Thus, it may be concluded that the energy method predicts the inertia effects reasonably accurately, in the range of application of SFDs, and this is true even for long dampers whose velocity profiles are more sensitive to Re. It is clear from Figure 8 that the inertia force is equal to the viscous force for Re=10, and is larger thereafter. In fact, the inertia force is about 4 times as large as the viscous force at Re = 40, and we can say that, at such high Re, the damper is totally dominated by the inertia forces.

The forces acting on the journal can be obtained by integrating equation (24), thus

$$F_r = -\int_{-\frac{L}{2}}^{\frac{L}{2}} \int_{\theta_1}^{\theta_2} p \cos\theta \; R \, d\theta \, dZ$$

$$F_t = -\int_{-\frac{L}{2}}^{\frac{L}{2}} \int_{\theta_1}^{\theta_2} p \sin\theta \; R \, d\theta \, dZ$$

Now using the limit of f(Re), equation (26), in equation (24), the forces acting on the journal become

$$F_r = 12\,\frac{\mu R^3 L}{c^3}\, e\,\omega \left\{ 1 - \frac{\tanh\left(\frac{L}{D}\right)}{\frac{L}{D}} \right\} \left[-\int_{\theta_1}^{\theta_2} \sin\theta \cos\theta \, d\theta + \frac{Re}{10}\int_{\theta_1}^{\theta_2} \cos^2\theta \, d\theta \right] \tag{27}$$

$$F_t = 12\,\frac{\mu R^3 L}{c^3}\, e\,\omega \left\{ 1 - \frac{\tanh\left(\frac{L}{D}\right)}{\frac{L}{D}} \right\} \left[-\int_{\theta_1}^{\theta_2} \sin^2\theta \, d\theta + \frac{Re}{10}\int_{\theta_1}^{\theta_2} \sin\theta\cos\theta \, d\theta \right] \tag{28}$$

where the quantity

$$K_L = \left\{ 1 - \frac{\tanh\left(\frac{L}{D}\right)}{\frac{L}{D}} \right\}$$

has been termed a leakage factor by Warner[11] which accounts for the finiteness of the damper. Equations (27) and (28) represent a finite length solution to the governing equations. To be able to compare the results of the kinetic coenergy method with the above equations, we have to consider the limiting cases of long and short dampers. For a long damper $L/D \rightarrow \infty$ thus $K_L \rightarrow 1$, and for a short damper $L/D \rightarrow 0$ thus $K_L \rightarrow \frac{1}{3}\left(\frac{L}{D}\right)^2$

For a long damper with 2π-film equations (27) and (28) become

$$F_r = 12\,\frac{\rho R^3 L}{10\,c}\,\pi\, e\,\omega^2 \tag{29}$$

$$F_t = -12\,\frac{\mu R^3 L}{c^3}\,\pi\, e\,\omega$$

The radial force is the centrifugal force and the tangential force is the damping force. These forces are the forces acting on the journal when it executes a small circular-centered orbit in a 2π-film. These are the same forces as those predicted by equation (12) for F_r and (13) for F_t, if we take the limit as ε tends to zero of the inertia and damping coefficients, which is the condition of a small orbit.

Similarly, for a short damper with 2π-film equations (27) and (28) become

$$F_r = \frac{\rho R L^3}{10\,c}\,\pi\, e\,\omega^2 \tag{30}$$

$$F_t = -\frac{\mu R L^3}{c^3}\pi e \omega$$

The radial force is the centrifugal force and the tangential force is the damping force. These forces are the forces acting on the journal when it executes a small circular-centered orbit in a 2π-film. These are the same forces as those predicted by equation (12) for F_r and (13) for F_t, if we take the limit as ε tends to zero of the inertia and damping coefficients, which is the condition of a small orbit. Thus it may be concluded that the forces acting on the journal when it executes a small circular-centered orbit in a squeeze film damper, obtained by taking the limit as $Re \rightarrow 0$ of the solution of the governing partial differential equations, are the same as those predicted by the kinetic coenergy method.

Equation (29), for a long damper, indicates that the radial force is proportional to the centrifugal acceleration, thus the proportionality constant represents the added mass to the journal m_{ad}

$$m_{ad} = 12\,\frac{\pi \rho R^3 L}{10\,c}$$

and the mass of the journal is m_j

$$m_j = \rho_{st}\,\pi R^2 L$$

where we assumed that the journal is made of steel and ρ_{st} is the density of steel. Then the ratio of the added mass to the mass of the journal is

$$\frac{m_{ad}}{m_j} = \frac{12}{10}\,\frac{\rho}{\rho_{st}}\,\frac{R}{c}$$

For typical SFDs, the ratio R/c is 1000 and the density of oil is approximately 800 kg/m^3, and the density of steel is approximately 7800 kg/m^3, then the added mass to the journal due to the oil film is approximately 60 times the mass of the journal. This is because of the huge velocities and accelerations that the fluid undergoes in a SFD.

Similarly, for a short damper, from equation (30), the added mass to the journal is

$$m_{ad} = \frac{\pi \rho R L^3}{10\,c}$$

and the ratio of the added mass to the mass of the journal is

$$\frac{m_{ad}}{m_j} = \frac{1}{10}\,\frac{\rho}{\rho_{st}}\,\frac{L^2}{R^2}\,\frac{R}{c}$$

If we assume R=L, and the typical values for the other parameters we used with the long dampers, then we find that the added mass to the journal due to the oil film is approximately 10 times the mass of the journal. The short dampers have a smaller added mass than the long dampers because the flow in the long dampers is the same at each section in the axial direction and thus every section is resisting the squeezing by the journal in the same manner, while for the short dampers the flow at each section in the axial direction varies linearly with the axial coordinate Z, and in fact is equal to zero at the middle of the damper. Thus the short dampers exhibit less resistance to the squeezing motion, and thus exhibit a smaller added mass.

Conclusion

Fluid inertia can be very important in squeeze film dampers. The added mass to the journal was shown to be as high as 60 times the mass of the journal, for small circular centered whirl, which cannot be neglected in the dynamic analysis of rotors incorporating squeeze film dampers. Also, for the case of small circular centered whirl, it was shown that the fluid inertia forces are equal to the viscous forces in the damper at squeeze Reynolds number equal to 10, and are larger thereafter.

Also it was shown that, for Reynolds number within the range of usual application of squeeze film dampers, the classical lubrication theory predicts the velocity profiles fairly accurately, which permits the kinetic coenergy of the fluid in the damper to be calculated. Finally it was shown that the fluid inertia forces predicted by the kinetic coenergy method are equal to those obtained by the solution of the governing equations for a small circular centered whirl.

References

[1] El-Shafei, A., "Dynamics of Rotors Incorporating Squeeze Film Dampers", Ph.D. Thesis, Department of Mechanical Engineering, Massachusetts Institute of Technology, Cambridge, MA, 1988.

[2] El-Shafei, A., "Unbalance Response of a Jeffcott Rotor Incorporating Short Squeeze Film Dampers", ASME paper 89 - GT - 75, 1989.

[3] Ramli, M.D., J. Ellis, and J.B. Roberts, "On the Computation of Inertial Coefficients in Squeeze-Film Bearings", Proc. I.Mech.E., Vol. 201, No. C2, 1987, pp. 125-131.

[4] Reinhardt, E., and J.W. Lund, "The Influence of Fluid Inertia on the Dynamic Properties of Journal Bearings", Journal of Lubrication Technology, Trans. ASME, Vol. 97, No. 2, 1975, pp.159-167.

[5] San Andrés, L.A. and J.M. Vance, "Effects of Fluid Inertia and Turbulence on the Force Coefficients for Squeeze Film Dampers", Journal of Engineering for Gas Turbine and Power, Trans. ASME, Vol. 108, No. 2, April 1986, pp. 332-339.

[6] San Andrés, L.A. and J.M. Vance, "Effect of Fluid Inertia on Squeeze-Film Damper Forces for Small-Amplitude Circular-Centered Motions", ASLE preprint 86 - AM - 3A - 3, 1986.

[7] Smith, D.M., "Journal Bearing Dynamic Characteristics - Effect of Inertia of Lubricant", Proc. I.Mech.E., 1964-1965, Vol. 179, pp. 37-44.

[8] Szeri, A.Z., A.A. Raimondi, and A. Giron-Durate, "Linear Force Coefficients of Squeeze Film Dampers", Journal of Lubrication Technology, Trans. ASME, 1983, pp. 326-334.

[9] Tecza, J.A., J.C. Giordano, E.S. Zorzi, and S.K. Drake, "Squeeze Film Damper Technology : Part 2 - Experimental Verification Using a Controlled Orbit Test Rig", ASME paper 83 - GT - 248, 1983.

[10] Tichy, J.A., "The Effect of Fluid Inertia in Squeeze Film Damper Bearings : A Heuristic and Physical Description", ASME paper 83 - GT - 177, 1983.

[11] Warner, P.C., "Static and Dynamic Properties of Partial Journal Bearings", Journal of Basic Engineering, Trans. ASME, June 1963, pp. 247-257.